

The characteristics of fluorinated gate dielectric AlGa_N/Ga_N MIS-HEMT

Minhan Mi¹, Yunlong He¹, Bin Hou², Meng Zhang², Zuochen Shi¹, Xiaohua Ma², Peixian Li^{2b)}, and Yue Hao^{1a)}

¹ Key Laboratory of Wide Bandgap Semiconductor Materials and Devices, School of Microelectronics, Xidian University, 2 South Taibai Road, 710071 Xi'an, P.R China

² School of Advanced Materials and Nanotechnology, Xidian University, 2 South Taibai Road, 710071 Xi'an, P.R China

a) yhao@xidian.edu.cn

b) pxli@mail.xidian.edu.cn

Abstract: In this letter, a normally-off AlGa_N/Ga_N MIS-HEMT using fluorinated gate dielectric was presented. The fluorine ions were injected into the Al₂O₃ gate dielectric to obtain positive threshold voltage (V_{th}) as well as avoiding the plasma induced to the Ga_N channel layer. Moreover the maximum transconductance of fluorinated gate MIS-HEMT has been improved compared with the non-treated MIS-HEMT. Furthermore, the fluorine ions injected into the Al₂O₃ gate dielectric could decrease the trap states density (D_T) and time constant (τ_T) at the Al₂O₃/Ga_N interface. The normally-off MIS-HEMT showed a very high drain current of 507 mA/mm and V_{th} of 0.6 V.

Keywords: Ga_N MIS-HEMT, normally-off, interface trap state

Classification: Electron devices, circuits, and systems

References

- [1] D. S. Lee, X. Gao, S. Guo, D. Kopp, P. Fay and T. Palacios: IEEE Electron Device Lett. **32** (2011) 1525. DOI:10.1109/LED.2011.2164613
- [2] A. Crespo, M. M. Bellot, K. D. Chabak, J. K. Gillespie, G. H. Jessen, V. Miller, M. Trejo, G. D. Via, D. E. Walker, Jr., B. W. Winningham, H. E. Smith, T. A. Cooper, X. Gao and S. Guo: IEEE Electron Device Lett. **31** (2010) 2. DOI: 10.1109/LED.2009.2034875
- [3] Y. F. Wu, A. Saxler, M. Moore, R. P. Smith, S. Sheppard, P. M. Chavarkar, T. Wisleder, U. K. Mishra and P. Parikh: IEEE Electron Device Lett. **25** (2004) 117. DOI:10.1109/LED.2003.822667
- [4] K. J. Chen and C. H. Zhou: Phys. Status Solidi A **208** (2011) 434. DOI: 10.1002/pssa.201000631
- [5] M. H. Mi, K. Zhang, X. Chen, Z. S. Zhao, C. Wang, J. C. Zhang, X. H. Ma and Y. Hao: Chin. Phys. B **23** (2014) 077304. DOI:10.1088/1674-1056/23/7/077304
- [6] W. Saito, Y. Tashiharu, M. Kuraguchi and I. Omura: IEEE Trans. Electron Devices **53** (2006) 356. DOI:10.1109/TED.2005.862708
- [7] L. Y. Su, F. Lee and J. J. Huang: IEEE Trans. Electron Devices **61** (2014) 460. DOI:10.1109/TED.2013.2294337

- [8] T. Inoue, T. Nakayama, Y. Ando, M. Kosaki, H. Miwa, K. Hirata, T. Uemura and H. Miyamoto: IEEE Trans. Electron Devices **55** (2008) 483. DOI:10.1109/TED.2007.912367
- [9] G. W. Li, T. Zimmermann, Y. Cao, C. X. Lian, X. Xing, R. H. Wang, P. Fay, H. G. Xing and D. Jena: IEEE Electron Device Lett. **31** (2010) 954. DOI:10.1109/LED.2010.2052912
- [10] Y. D. Du, W. H. Han, W. Yan and F. H. Yang: Chin. Phys. Lett. **31** (2014) 048501. DOI:10.1088/0256-307X/31/4/048501
- [11] S. L. Zhao, J. S. Xue, P. Zhang, B. Hou, J. Luo, X. J. Fan, J. C. Zhang, X. H. Ma and Y. Hao: Appl. Phys. Express **7** (2014) 071002. DOI:10.7567/APEX.7.071002
- [12] P. D. Ye, B. Yang, K. K. Ng and J. Bude: Appl. Phys. Lett. **86** (2005) 063501. DOI:10.1063/1.1861122
- [13] C. Chen, X. Z. Liu, B. L. Tian, P. Shu, Y. F. Chen, W. L. Zhang, H. C. Jiang and Y. R. Li: IEEE Electron Device Lett. **32** (2011) 1373. DOI:10.1109/LED.2011.2162933
- [14] S. Yang, S. Huang, M. Schnee, Q. T. Zhao, J. Schubert and K. J. Chen: IEEE Trans. Electron Devices **60** (2013) 3040. DOI:10.1109/TED.2013.2277559
- [15] Y. Y. Lu, S. Yang, Q. M. Jiang, Z. K. Tang, B. K. Li and K. J. Chen: Phys. Status Solidi **10** (2013) 1397. DOI:10.1002/pssc.201300270
- [16] S. L. Zhao, K. Zhang, W. Ha, Y. H. Chen, P. Zhang, J. C. Zhang, X. H. Ma and Y. Hao: Appl. Phys. Lett. **103** (2013) 212106. DOI:10.1063/1.4832482

1 Introduction

Wide band-gap III-nitride semiconductor materials possess many superior material properties than conventional Si, GaAs or any other III-V compounds. The major advantages of the III-nitride devices are high-power, high-frequency and high-temperature due to their excellent properties, such as high breakdown electric field, high saturation and high sheet concentrations at heterojunction [1, 2, 3]. However, there still remains much to be solved for III-nitride, particularly for the normally-off operation, in terms of achieving low-cost, high-efficiency and simple circuit configuration and improving the circuit reliability [4]. Several advanced processing schemes to achieve normally-off operation have been applied to the AlGaIn/GaN HEMTs, such as using a thin AlGaIn barrier layer [5], a recessed gate structure [6], a p-type gate structure [7], piezoelectric neutralization technology [8] in combination with high work function metal gates [9] and a fluoride-based plasma treatment to maximize V_{th} [10]. However, the drain current reductions are significantly range from 24%~80% comparing with the untreated devices at the same $V_{GT} = V_G - V_{th}$ [11].

In this work, we adopt an Al_2O_3 layer deposited by atomic layer deposition (ALD) as the barrier to prevent implantation of fluorine ions into the AlGaIn/GaN heterostructure. Unlike the conventional fluorine ions directly injected the AlGaIn barrier layer which causes plasma-induced damage to AlGaIn barrier and AlGaIn/GaN heterostructure that degrade the electron mobility and increase the gate leakage current. The injected F ions act as negative charges in the Al_2O_3 layer which lead to the reduction of 2DEG density under the gate. Therefore fluorinated gate AlGaIn/GaN MIS-HEMT achieve positively move V_{th} without degradation in

2DEG channel mobility. Besides, we found an interesting phenomenon that the V_{th} hysteresis of F injected MIS-HEMT has been greatly decreased. In order to find out the reason, the frequency conductance analysis was adopted to investigate the interface trap states between the dielectric and barrier.

2 Device structure and fabrication

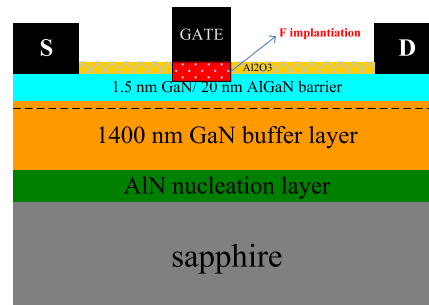


Fig. 1. Schematic cross section of fluorinated gate dielectric AlGaIn/GaN MIS-HEMT.

The sample used in this work was grown on sapphire substrate by metal-organic chemical vapor deposition (MOCVD). The schematic cross section of the fluorinated gate dielectric AlGaIn/GaN MIS-HEMT is shown in Fig. 1. The epitaxial layers consisted of, from bottom to top, a low-temperature AlN nucleation layer, a 1.4- μm unintentionally doped GaN buffer layer, a 20-nm AlGaIn barrier layer with an Al mole fraction of 30% followed by a 1.5-nm GaN cap layer. Adding a GaN cap layer to the AlGaIn/GaN structure can reduce the ohmic contact resistance. Room-temperature Hall measurements showed an electron sheet concentration of $1 \times 10^{13} \text{ cm}^{-2}$ and a mobility of $1960 \text{ cm}^2/\text{Vs}$, resulting in a sheet resistance of $317 \Omega/\square$.

The device fabrication started with the formation of source/drain contact consisting of Ti/Al/Ni/Au (22 nm/140 nm/55 nm/45 nm) by electron beam evaporation and annealed in N_2 ambient at 830°C for 30 s. Then, a 120 nm mesa etched by Cl_2 -based reactive ion etching (RIE) was used as a device region. The buffer leakage was $6.57 \times 10^{-6} \text{ mA/mm}$ between two isolated mesas at a distance of 5- μm and the voltage across the two isolated mesas was 100 V. Using on-wafer transfer length method (TLM), the ohmic contact resistance was measured to be $0.4 \Omega\cdot\text{mm}$. A 10 nm Al_2O_3 film deposited by atomic-layer-deposited (ALD) was used as the surface passivation and gate dielectric simultaneously [12]. This could simplify the fabrication process. After gate windows with 1.2- μm length were opened by photolithography, the gate dielectric was treated with CF_4 plasma in an RIE system. Finally a Ni/Au/Ni (45 nm/200 nm/20 nm) gate electrode was deposited by electron beam evaporation. The F injected treatment and the gate region was defined by the same mask as well as self-aligned. Devices without F injected treatment were also fabricated on the same wafer for comparison. All the devices in this paper have a gate length of 1.2- μm , a source-drain spacing of 4- μm and a gate-drain spacing of 2.1- μm . For convenience, fluorinated gate dielectric AlGaIn/GaN HEMT was called F injected MIS-HEMT while the non-treated gate dielectric AlGaIn/GaN HEMT was MIS-HEMT.

3 Results and discussion

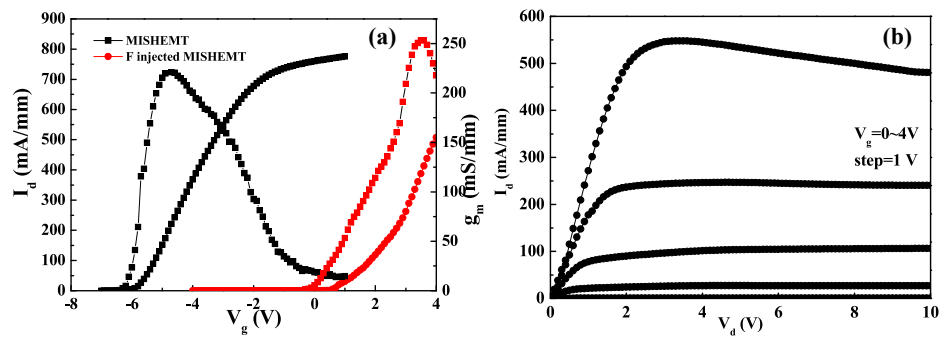


Fig. 2. (a) Transfer characteristics and (b) output characteristics.

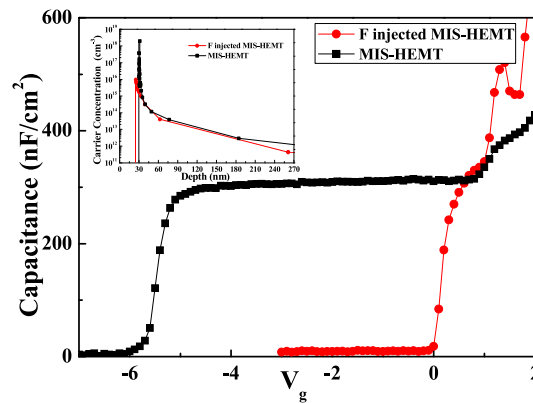


Fig. 3. C-V characteristics of F injected MIS-HEMT and MIS-HEMT. Inset shows electrons distribution with depth for F injected MIS-HEMT and MIS-HEMT.

Fig. 2(a) plots the transfer characteristics of MIS-HEMT and F injected MIS-HEMT. We define V_{th} as the gate bias intercept of the linear extrapolation of drain current at the point of peak transconductance (g_m). The value of V_{th} is 0.6 V for F injected MIS-HEMT, corresponding to a V_{th} shift of +6.1 V from the MIS-HEMT. The values of drain current (I_d) are 507 mA/mm and 600 mA/mm for F injected MIS-HEMT and MIS-HEMT at the same $V_{GT} = 3.4$ V. And the maximum I_d of F injected MIS-HEMT has not saturated. Due to the large gate leakage current, otherwise the gate voltage of F injected MIS-HEMT can continue to improve therefore maximum drain current can also increase. The peak g_m of MIS-HEMT is 220 mS/mm. In contrast, the peak g_m of F injected MIS-HEMT is 253 mS/mm due to fluorine ions accumulation only in the dielectric and no penetration into AlGaIn/GaN heterostructure [13]. There are two reasons for the increased peak g_m . One is F injected treatment induced dielectric thinning that decreases the separation between the gate electrode and 2DEG. After the F injected treatment, the thickness of dielectric is 5 nm which can be confirmed from electrons distribution curve in Fig. 3. The other reason is explained below. Because accurate capacitance measurement requires low gate leakage, the positive gate voltage is limited to 2 V as shown in Fig. 3. Gate leakage current characteristics are shown in Fig. 4(a). Under a positive gate bias $V_g = 4$ V, the gate leakage current (I_g) of F injected MIS-HEMT and MIS-HEMT is 1.9 mA/mm and 0.037 mA/mm respectively. It is observed that

the gate leakage current of F injected MIS-HEMT is only two orders of magnitude larger than that of MIS-HEMT. The reason for the increase of gate leakage is F injection process can slightly etch the dielectric layer which causes dielectric thinning. However, the leakage current of F injected MIS-HEMT still lower than HEMT by two orders of magnitude. The breakdown voltage V_{br} is measured at $V_g = 0$ V for F injected MIS-HEMT and $V_g = -10$ V for MIS-HEMT. And the V_{br} is defined as the voltage at which the drain current I_d reaches 1 mA/mm. The breakdown voltages are 121 V and 83 V for F injected MIS-HEMT and MIS-HEMT as shown in Fig. 4(b). It can be seen that the breakdown of both devices are induced by buffer leakage because the drain current is acted as the dominated role in the whole breakdown process. This suggest that the thinning of dielectric thickness caused by plasma is finite and the F injected MIS-HEMT can meet the requirement for normally-off mode operation because the gate leakage current is still sufficiently low. We suppose that F injected MIS-HEMT has a larger breakdown voltage mainly because of injected F ions in the dielectric layer and dielectric/GaN interface can extend the depletion region under the gate area toward the substrate direction, thus reducing the buffer leakage with a narrower leakage current path [11].

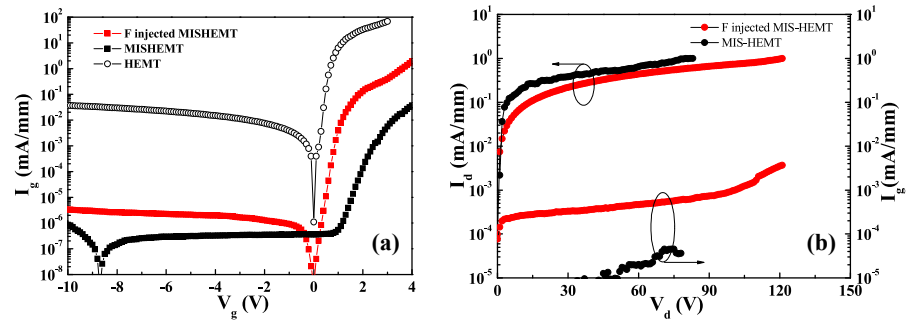


Fig. 4. (a) Gate leakage current characteristics and (b) DC breakdown characteristics.

To investigate the trap state at the dielectric/GaN interface, the transfer characteristics are measured in double-sweep mode with different V_D from 0.5 V to 2 V. The small drain voltage is selected to avoid the field assisted de-trapping effect [14]. When V_g is swept from closed bias to positive bias, electrons can spill over from AlGaIn/GaN heterostructure to the dielectric/GaN interface, and fill up the interface states below the Fermi level. As the V_g sweep back to the closed bias, fast traps can emit electrons during the sweep period, thus cannot introduce V_{th} hysteresis. Whereas slow traps are still filled with electrons, resulting in V_{th} hysteresis [15]. It can be seen from Fig. 3 that the 2DEG spill over occurs when the gate voltage reach +1 V in both F injected MIS-HEMT and MIS-HEMT. Therefore, the positive gate bias is selected to be +2 V to cause 2DEG spill over. In the Fig. 5, the V_{th} hysteresis only slightly increases from 90 mV to 120 mV for F injected MIS-HEMT when the V_D are decreased from 2 V to 0.5 V, which is much lower than the MIS-HEMT. Based on the results, we can qualitatively estimate either the density of trap states or the time constant of trap states has been decreased by F injected treatment.

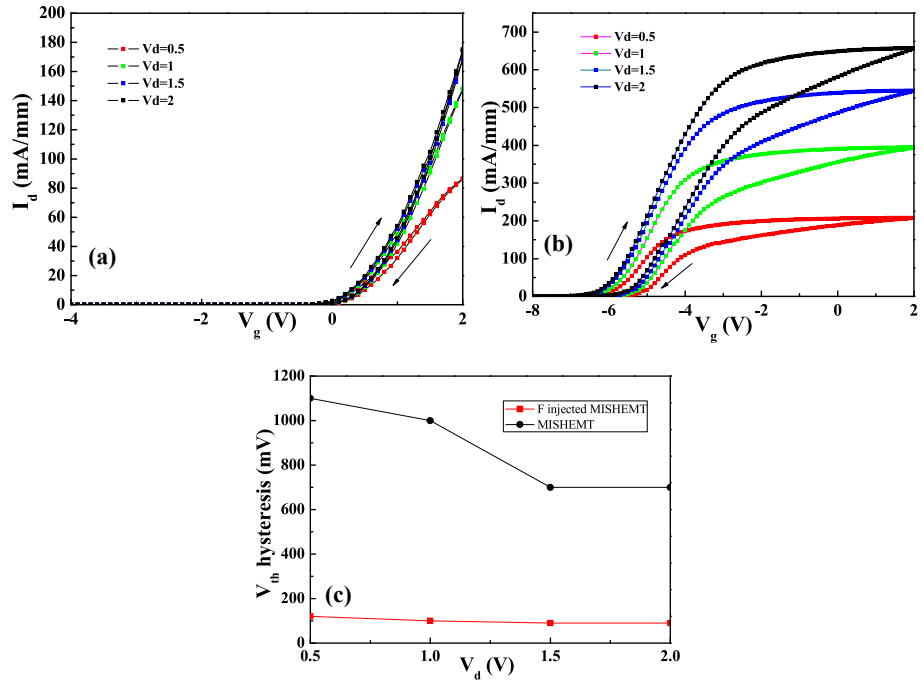


Fig. 5. Transfer sweep measured with different V_D from 0.5 V to 2 V of (a) F injected MIS-HEMT and (b) MIS-HEMT. (c) Comparison of V_{th} hysteresis of F injected MIS-HEMT and MIS-HEMT varied with different V_D .

In order to quantitatively investigate the trap states at dielectric/GaN interface before and after the fluorine ions injected into gate dielectric, we conduct frequency dependent conductance measurements to study the variations of trap state [16]. The device gate bias should be biased at the positive voltage accumulation region which insures the 2DEG spill over so that only trap states at dielectric/GaN interface can respond to the measurement signal. 2DEG spill over in both devices occurs at the gate voltage around the 0.8 V. Therefore the gate bias is selected from 0.5 V to 1.1 V for all the devices. Fig. 6 shows G_p/ω versus ω for the two devices at selected gate voltage. The trap states density D_T and the time constant τ_T could be extracted by fitting the measured parallel conductance G_p as a function of ω according to equation $G_p/\omega = (qD_T/2\omega\tau_T) \ln[1 + (\omega\tau_T)^2]$, where $\omega = 2\pi f$ is the radial frequency, G_p/ω has a maximum value $\omega = 2/\tau_T$ and at that maximum $D_T = 2.5G_p/q\omega$. The variations of time constant trap state with gate voltage, assessed for the two devices, are shown in Fig. 7(a). The trap time constant $\tau_T = 0.31 \mu s \sim 0.55 \mu s$ for F injected MIS-HEMT and $\tau_T = 0.36 \mu s \sim 0.92 \mu s$ for MIS-HEMT. The trap state energy E_T could be found using the time constant resulting from the fitting procedure and considering that $\tau_T = (\sigma_T N_c v_T)^{-1} \exp(E_T/kT)$, where the capture cross section of the trap state $\sigma_T = 3.4 \times 10^{-15} \text{ cm}^2$, the density of states in the conduction band $N_c = 2.2 \times 10^{18} \text{ cm}^{-3}$, and the average thermal velocity of the carriers $v_T = 2.6 \times 10^{17} \text{ cm/s}$ are used. For MIS-HEMT, trap state density of $1.9 \times 10^{13} \sim 4.1 \times 10^{13} \text{ cm}^{-2} \text{ eV}^{-1}$ are located at E_T in a range of 0.29~0.315 eV. In contrast, trap state density of $3.4 \times 10^{12} \sim 6.3 \times 10^{12} \text{ cm}^{-2} \text{ eV}^{-1}$ are located at E_T in a range of 0.287~0.301 eV for F injected MIS-HEMT. It is noted that F injected into dielectric under the gate decreases the density of trap state at dielectric/GaN interface nearly one order of magnitude. And the time constant of

trap state also has been reduced slightly. The results provide evidence for the decreased V_{th} hysteresis because of the lower density of trap state at the dielectric/GaN interface. Although the increase of peak g_m could be attributed to the gate dielectric layer thinning by F injected treatment, the main reason is the decreasing of trap state, consequently enhancing the ability to control the gate of the channel. Therefore, it is believed that F injected into the dielectric can passivate the trap state at dielectric/GaN interface.

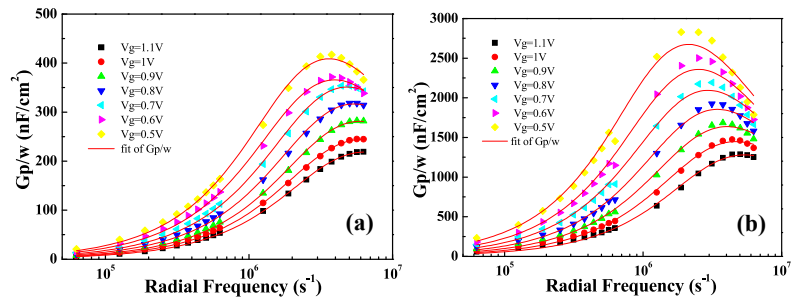


Fig. 6. Variations of conductance with radial frequency for (a) F injected MIS-HEMT and (b) MIS-HEMT at selected gate voltages.

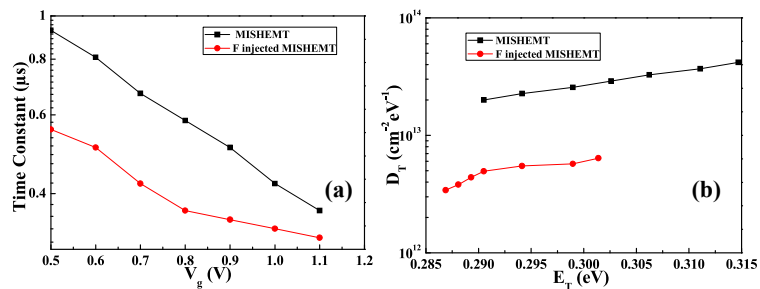


Fig. 7. (a) Plots of trap state time constant versus gate voltage and (b) plots of trap state density versus energy for F injected MIS-HEMT and MIS-HEMT.

4 Conclusion

In summary, this work demonstrates fluorinated gate dielectric AlGaN/GaN MIS-HEMT. The fluorine ions directly injected into the dielectric realizes the normally off mode MIS-HEMT with improved breakdown voltage. Besides, the injected fluorine ions can passivate the trap state at dielectric/GaN interface so that the reduced V_{th} hysteresis obtained. This results show the method of F injected into the gate dielectric has the great potential to realize the high performance normally off mode operation.

Acknowledgments

This work was supported by the National Natural Science Foundation of China (Grant Nos. 61334002 and 61106106) and the Opening Project of Science and Technology on Reliability Physics and Application Technology of Electronic Component Laboratory (Grant No. ZHD201206).